Some comments on Hijing B-Bbar

Rene Bellwied (University of Houston)

I am not the expert, but I asked Prithwish a pointed question at the APS Meeting.

I worked with Vasile Topor-Pop in the early 2000s on baryon junctions as a way of describing hyperon enhancement.

Fundamental Work:
1.) G.C. Rossi and G. Veneziano, Nucl. Phys. B123, 507 (1977); Phys. Rep. 63, 153 (1980)
2.) D. Kharzeev, Phys. Lett. B 378, 238 (1996)

HIJING B-Bbar:
3.) S.E. Vance, M. Gyulassy, and X.N. Wang, Phys. Lett. B443, 45 (1998)
4.) S.E. Vance, M. Gyulassy, Phys. Rev. Lett. 83, 1735 (1999)
5.) I. Vitev, M. Gyulassy, PRC65, 041902® (2002)
6.) V. Topor Pop, M. Gyulassy, J. Barrette, C. Gale, X.N. Wang, N. Xu, and K. Filimonov, *Phys.Rev. C* 68, 054902 (2003)
7.) V. Topor Pop, M. Gyulassy, J. Barrette, C. Gale, X. N. Wang, N. Xu, *Phys.Rev.C* 70, 064906 (2004)
8.) V. Topor Pop, M. Gyulassy, J. Barrette, C. Gale, R. Bellwied, *Phys.Rev.C* 72 (2005) 054901

Baryon junctions

The idea that nonperturbative three color flux junctions could play an important role in baryon and anti-baryon production at high energies was proposed long ago by Rossi and Veneziano on the basis of dual regge theory. This idea was extended and applied by Kharzeev to nuclear collisions.

Unlike conventional diquark fragmentation models, a baryon junction allows the diquark to split with the three independent flux lines tied together at a junction.

The main reason for baryon junctions at the time: the p/π anomaly at mid-p_T

PHYSICAL REVIEW C, VOLUME 65, 041902(R)

Jet quenching and the $\bar{p} \gtrsim \pi^-$ anomaly in heavy ion collisions at relativistic energies

Ivan Vitev[1] and Miklos Gyulassy[1,2]
[1]*Department of Physics, Columbia University, 538 West 120th Street, New York, New York 10027*
[2]*Collegium Budapest, Szentharomsag u.2, H-1014 Budapest, Hungary*
(Received 3 May 2001; published 3 April 2002)

PHENIX data on Au+Au at $\sqrt{s}=130A$ GeV suggest that $\bar{p}$ yields may exceed π^- at high p_T >2 GeV/c. We propose that jet quenching in central collisions suppresses the hard PQCD component of the spectra in central $A+A$ reactions, thereby exposing a novel component of baryon dynamics that we attribute to (gluonic) bayron junctions. We predict that the observed $\bar{p} \gtrsim \pi^-$ and the $p > \pi^+$ anomaly at $p_T \sim 2$ GeV/c is limited to a finite p_T window that decreases with increasing impact parameter.

Baryon and antibaryon production may in fact dominate the moderate high p_T hadron flavor yields, a phenomenon never before observed.

The assumption, in contrast to recombination models, is that strings survive and propagate

An attractive dynamical model that explains copious midrapidity baryon and antibaryon production is based on the existence of topological gluon field configurations (baryon junctions).

Other relevant measurements

Besides *mid-p_T baryon enhancement* other measurements point to novel baryon transport dynamics playing role in nucleus-nucleus (AA) reactions.

STAR data revealed a high *valence proton rapidity density (~10), five units from the fragmentation regions, and a pbar/p=0.65 at midrapidity.*

Junctions predict long-range baryon number transport in rapidity as well as *hyperon enhancement (including Ω^-)* and considerable p_T relative to conventional diquark-quark string fragmentation (large anti-hyperon enhancement at SPS energies).

Dima’s mechanism

The baryon transport mechanism suggested in [9] predicts that the valance baryon number per unit rapidity has the form

$$\frac{dN^B}{dy} \simeq \frac{dN^p}{dy} - \frac{dN^{\bar{p}}}{dy} = \beta Z \frac{\cosh(1-\alpha_B(0))y}{\sinh(1-\alpha_B(0))Y_{\max}}, \qquad (4)$$

where $\alpha_B(0) \simeq 1/2$ is the baryon junction exchange intercept. For Au+Au reactions at $\sqrt{s} = 130A$ GeV Eq. (4) predicts $dN^B/dy \simeq 10$ which is in good agreement with RHIC data [7].

Baryon anomaly ($p/\pi > 1$) at mid p_T

One important feature of HIJING is that it can account for the pion quenching component of the baryon anomaly. However, the LUND JETSET di-quark string fragmentation mechanism used in HIJING v1.37 completely fails to describe the baryon spectra observed in A+A collisions at all energies. HIJING/B and HIJING/BBbar1.10 were developed to address this failure at SPS energies.

Both were however also found to be inadequate with respect to baryon observables.

HIJING 1.37

In HIJING1.37 [38] the soft beam jet fragmentation is modeled by diquark-quark strings as in [39] with gluon kinks induced by soft gluon radiations. The mini-jets physics is computed via an eikonal multiple collision framework using pQCD PYTHIA5.3 to compute the initial and final state radiation and hard scattering rates. The cross section for hard parton scatterings is enhanced by a factor K=2 in order to simulate high order corrections. HIJING extends PYTHIA to include a number of new nuclear effects. Besides the Glauber nuclear eikonal extension, shadowing of nuclear parton distributions is modeled. In addition dynamical energy loss of the (mini)jets is taken into account through an effective dE/dx.

Single baryon junction vs JJbar loops, Vance1998

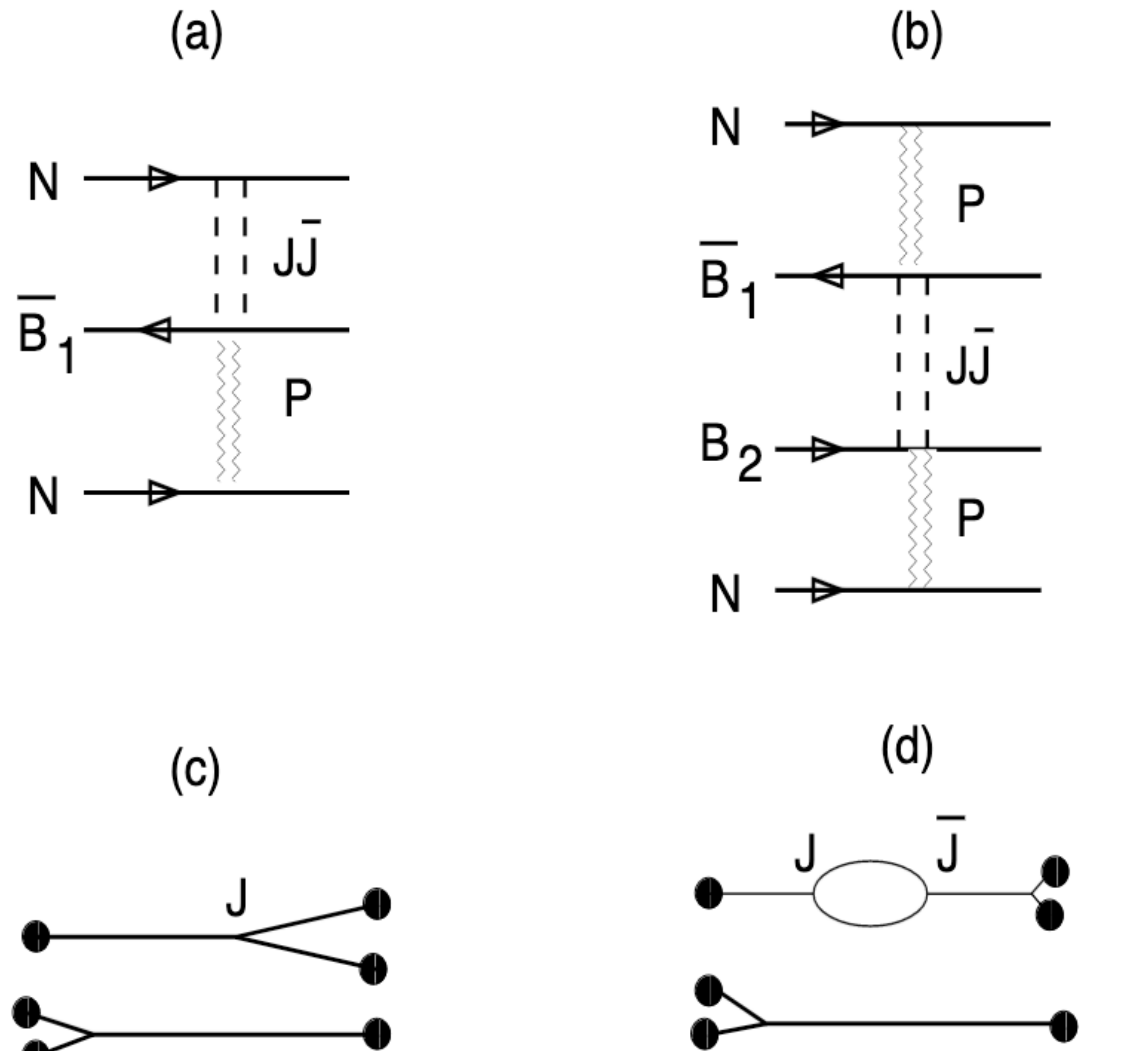

FIG. 1. The Regge diagrams for the single baryon junction exchange and $J\bar{J}$ loops are shown in (a) and (b), respectively. The string model implementation of each Regge diagram are shown in (c) and (d).

HIJING/B HIJING/BBar

Difference between HIJING and HIJING/B at SPS energies (Vance et al.,1998)

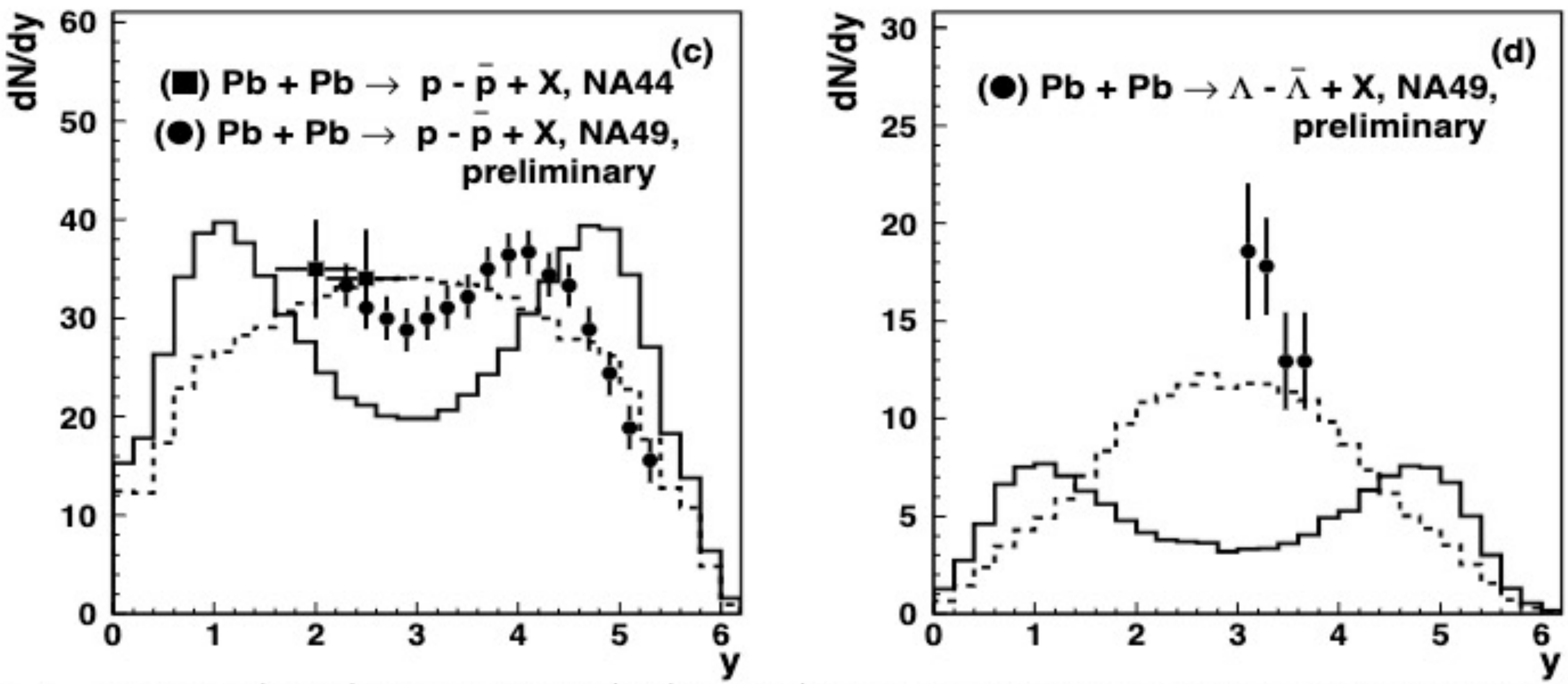

FIG. 1. HIJING (solid) and HIJING/B (dashed) calculations of the valence proton and hyperon rapidity distributions are shown for minimum bias $p+S$ collisions at 200 AGeV and central $Pb+Pb$ collisions at 160 AGeV. The data are from measurements made by the NA35 [1,2], NA44 [3] and NA49 [5] collaborations.

Difference between HIJING and HIJING/B at SPS/RHIC energies (Vance et al.,1998/1999)

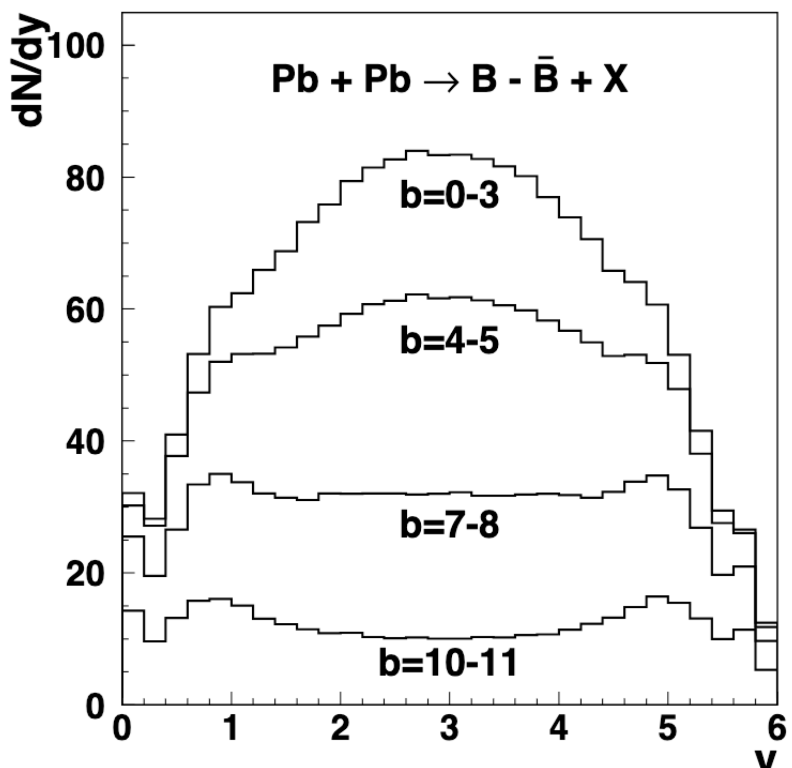

FIG. 2. Calculations of the net valence baryon rapidity distributions using HIJING/B are given for the impact parameter windows of $b = 0-3$ fm, $b = 4-5$ fm, $b = 7-8$ fm and $b = 10-11$ fm. In this calculation, the net valence baryons are defined as $B-\bar{B} = (p-\bar{p}) + (n-\bar{n}) + (\Lambda-\bar{\Lambda})$.

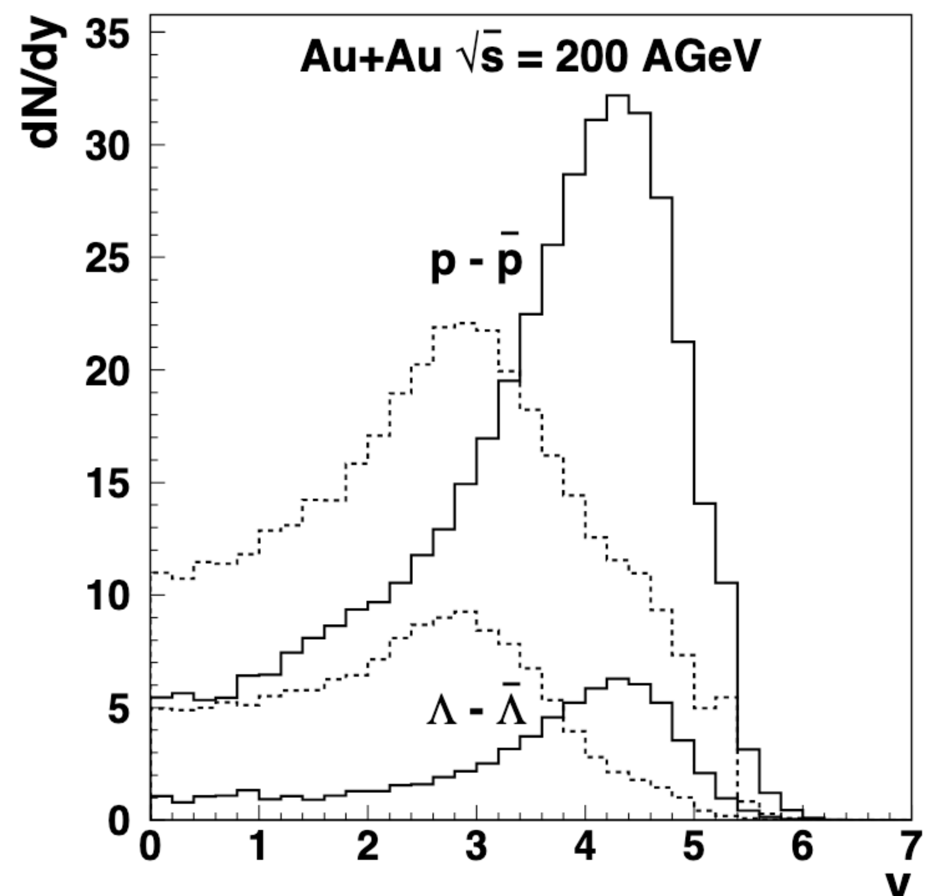

FIG. 3. Predictions for the initial valence proton rapidity distribution (upper two curves) and for the initial valence hyperon rapidity distribution (lower two curves) are given for Au+Au collisions at $E_{cm} = 200$ AGeV by HIJING (solid) and HIJING/B(dashed).

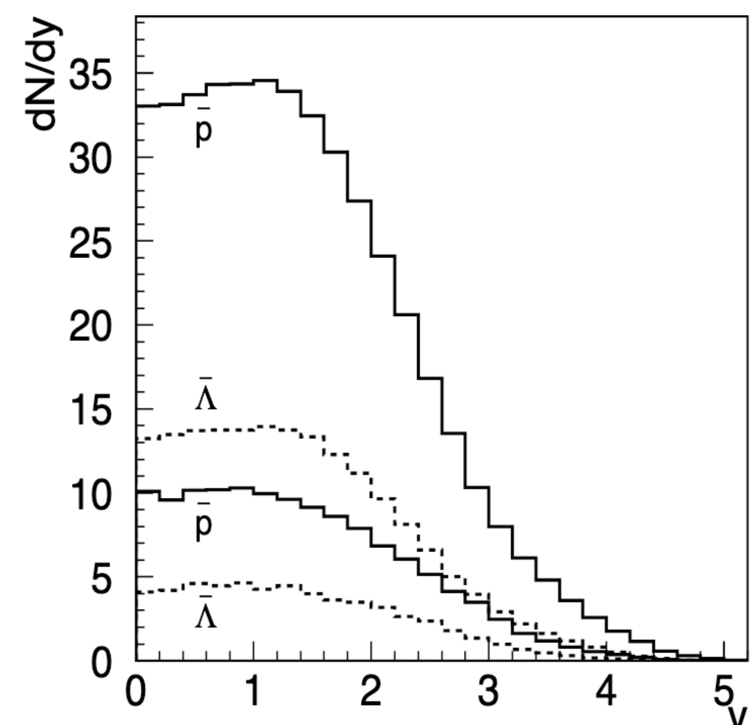

FIG. 4. Predictions for the initial $\bar{p}$ (solid lines) and $\bar{\Lambda}$ (dashed lines) rapidity distributions are given for HIJING (upper solid and dashed curves) and for HIJING/B$\bar{\text{B}}$ (lower solid and dashed curves) for Au+Au collisions at $E_{cm} = 200$ at $b \leq 3$ fm.

HIJING/BBbar v1.10

In HIJING/B$\bar{\text{B}}$ v1.10 [13] the baryon junction mechanism was introduced as an extension of HIJING/B [17] in order to try to account for the observed longitudinal distributions of baryons(B) and anti-baryons($\bar{\text{B}}$) in proton nucleus (p+A) and nucleus-nucleus (A+A) collisions at the SPS energies. However, as implemented in HIJING/B$\bar{\text{B}}$v1.10 the junction loops still fail to account for the observed transverse slopes of anti-baryons at moderate p_T as shown in [42]. This motivated us to try to reformulate the junction loop implementation in the present HIJING/B$\bar{\text{B}}$ (v2.0).

Impact on Rapidity distribution (PRC68, 054902, (2003))

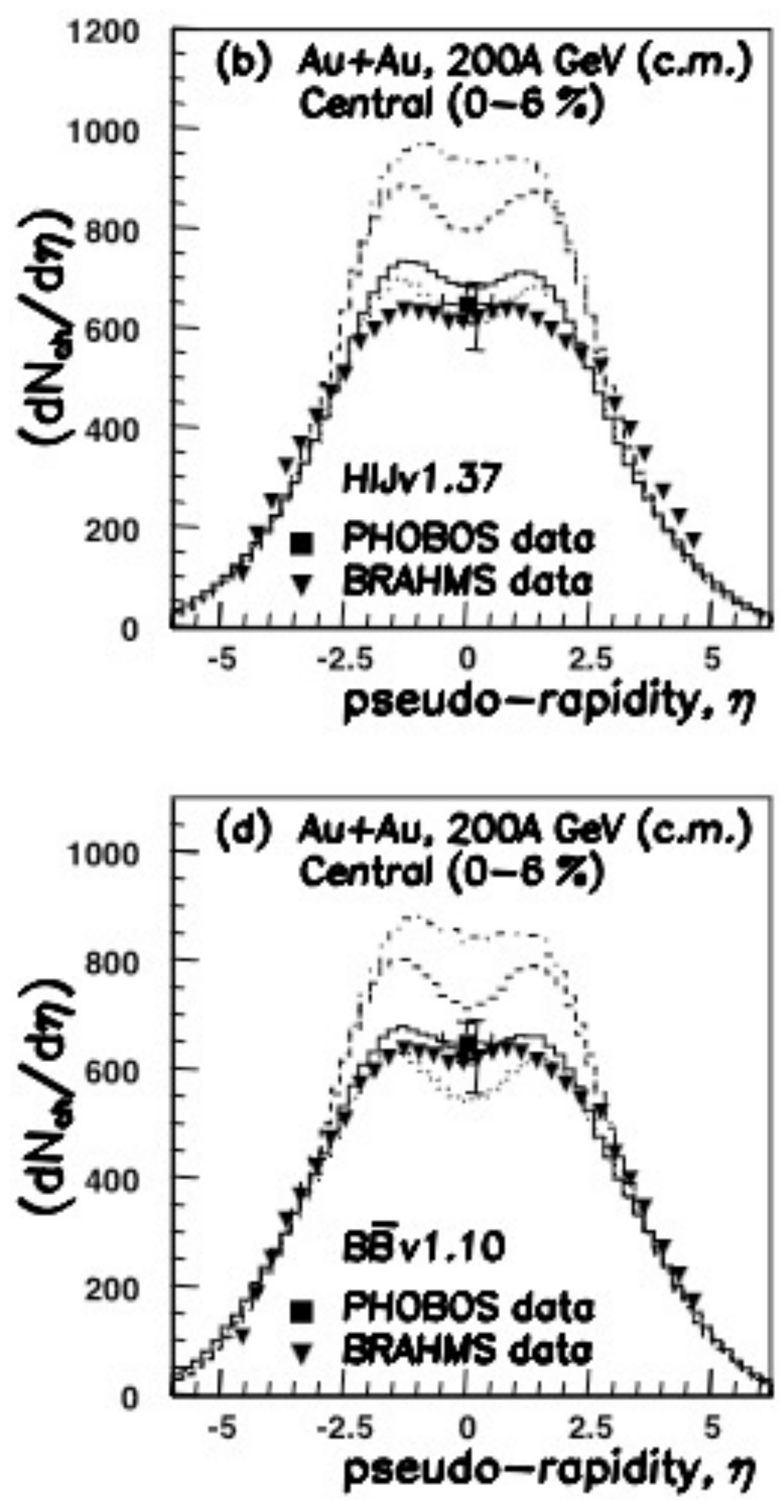

FIG. 1. Charged hadron rapidity distributions for central (0–6%) Au+Au collisions as function of c.m. energies. The histograms show the theoretical predictions from HIJING v1.37 (upper part) and HIJING/$B\overline{B}$ v1.10 (lower part) with (y) or without (n) effects of quenching q or/and shadowing s included. The data are from PHOBOS Collaboration [26] (a), [27] (b), [28] (c), and BRAHMS Collaboration [33] (c). The error bars at midrapidity include systematic uncertainties. The other error bars of the order of 10–15% have been omitted for clarity.

Vance et al.: Hyperons, 1999

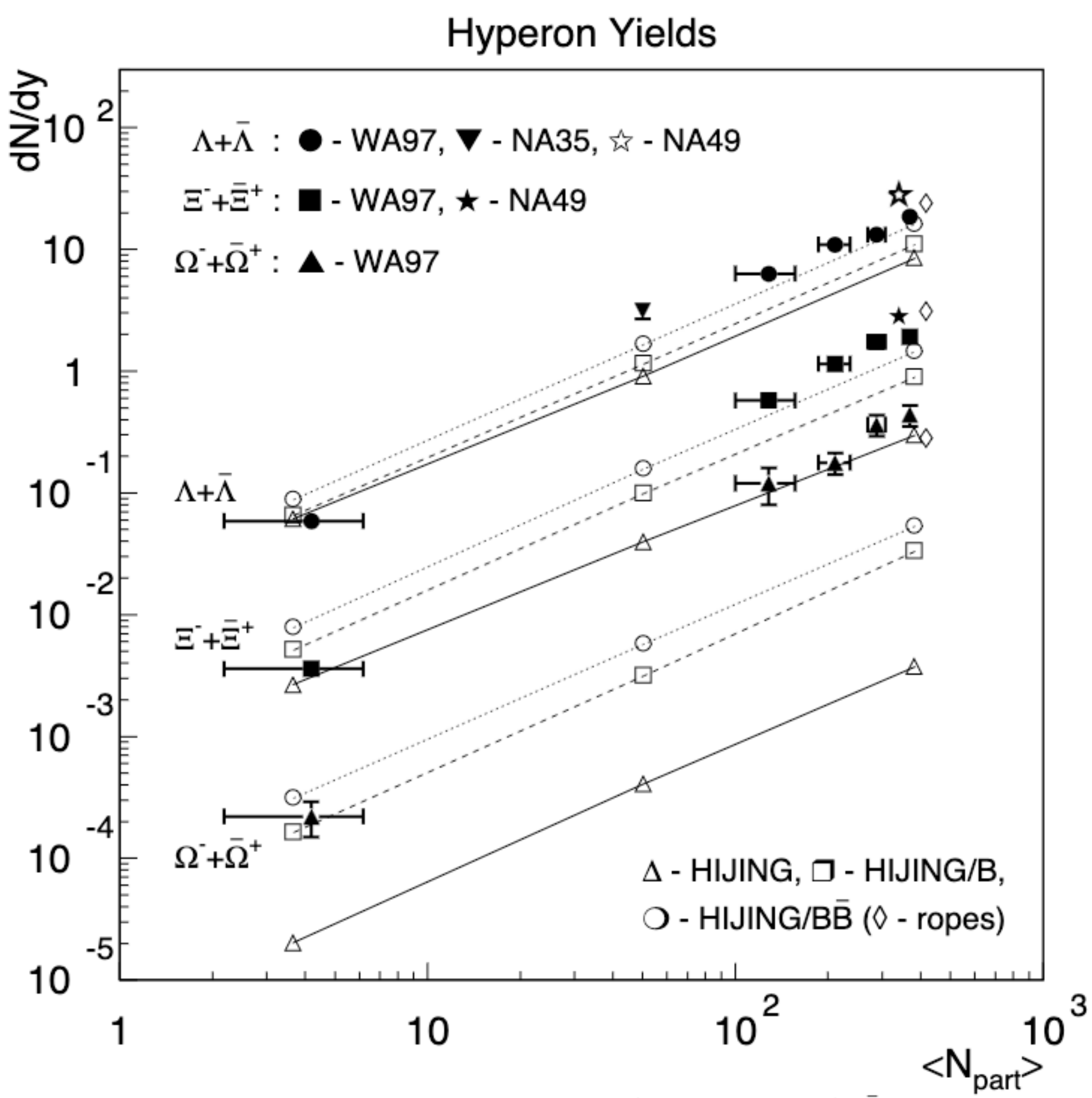

FIG. 2. Hyperon yields from HIJING, HIJING/B and HIJING/$B\bar{B}$ for $p + Pb$, $S + S$ and $Pb + Pb$ at incident momentum $p_{lab} = 160$ AGeV are shown along with data from the NA35 [26], the NA49 [2,3] and the WA97 [1] collaborations.

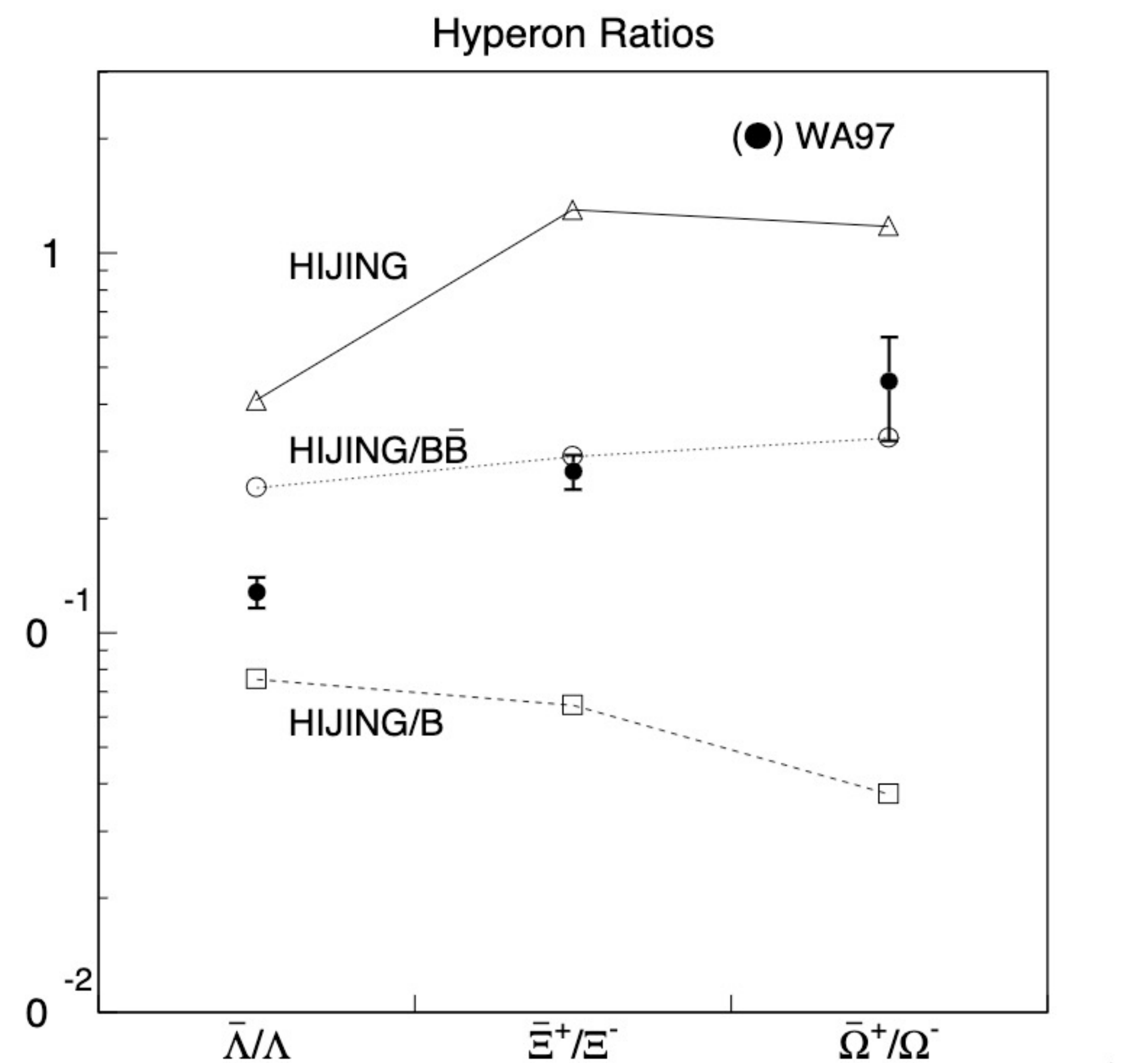

FIG. 3. The ratios of the yields of antihyperons to hyperons are shown for HIJING, HIJING/B d HIJING/$B\bar{B}$ for $p + Pb$, $S + S$ and $Pb + Pb$ at incident momentum $p_{lab} = 160$ AGeV along ith data from the WA97 [1] collaboration.

HIJING/BBbar v2.0

The $J\bar{J}$ loop algorithm of v1.10 has been replaced by a simple enhancement of the intrinsic (anti)diquark p_T kicks in any string that has been selected to contain one or more loops. Multiple hard and soft interactions proceed as in HIJING1.37. Before fragmentation however via JETSET we compute the probability that a junction loop occurs in the string. A picture of a juction loop is as follows: a color flux line splits at some intermediate point into two flux line at one junction and then the flux line fuse back into one at a second anti-junction somewhere further along the original flux line. The distance in rapidity between these points is chosen via a Regge distribution as described bellow. For single inclusive baryon observables this distribution does not need to be specified.

The probability of such a loop is assumed to increase with the number of binary interactions, n_{hits} that the incident baryon suffers in passing through the oncoming nucleus. This number depends on the relative and absolute impact parameters and is computed in HIJING using the eikonal path through a diffuse nuclear density.

HIJING/BBbar v2.0

The production of a baryon and antibaryon from a $J\bar{J}$ loop is simulated via an enhancement of the diquark p_T kick parameter $\sigma_{qq} = PARJ(21)$ of JETSET7.3. The default value is $\sigma_{qq} = 0.36$ GeV/c in ordinary string fragmentation. However in events where the string has a junctions loop we can expect a significantly higher p_T kick [13]. We therefore propose a very simple algorithm whereby the $J\bar{J}$ is modeled by enhancing σ_{qq} by a factor F_{p_T} which we fit to best reproduce the observed p_T spectrum of the baryons. This implementation of the $J\bar{J}$ model marks a radical departure from that implemented in HIJING/B$\bar{\text{B}}$v1.10.

While the above model allows the baryon antibaryon pairs to acquire much high transverse momentum in accord with observation, the absolute production rate also depends on the diquark/quark suppression factor $PARJ(1)$. The JETSET default for ordinary (fundamental flux) strings has $PARJ(1) = 0.1$. The reduced number of protons and anti protons observed at RHIC relative to HIJING1.37, will be shown below to be accounted for, if PARJ(1) is reduced to 0.07 in $J\bar{J}$ loops.

Modified fragmentation

We parametrize the soft phenomenological component of moderate p_T hadrons as follows:

$$\frac{dN_s(\mathbf{b})}{dy d^2\mathbf{p}_T} = \sum_{\alpha=\pi,K,p,\dots} \frac{dn^\alpha}{dy}(\mathbf{b}) \frac{e^{-p_T/T^\alpha(\mathbf{b})}}{2\pi(T^\alpha(\mathbf{b}))^2}. \quad (3)$$

As in string models the soft component is assumed to scale with the number of participants (N_{part}). In Eq. (3) we also account for the possibly different mean inverse slopes T^α for baryons and mesons. In the junction picture [8], the large $T^{\bar{p}}$ may arise from the predicted [9] smaller junction trajectory slope $\alpha'_J \approx \alpha'_R/3$. This implies that the *effective* string tension is three times higher than $1/(2\pi\alpha'_R) \approx 1$ GeV/fm leading in the massless limit to $\langle p_T^2 \rangle_J \simeq 3\langle p_T^2 \rangle_R$. In terms of the string model the factor three enhancement of the mean square p_T is due to the random walk in p_T arising from the decay of the three strings attached to the junction. Naively, we would thus expect $T^p \simeq \sqrt{3} T^{\pi^-}$. In a detailed Monte Carlo study [22] using HIJING/B$\bar{\text{B}}$ [9] this relation was indeed found to hold in the $1 \leq p_T \leq 2$ GeV/c range with $T^\pi \approx 220$ MeV and $T^p \approx 370$ MeV $\sim \sqrt{3} T^\pi$ with junctions included and $T^p \sim 270$ MeV without. At higher p_T the PQCD minijets cause the apparent pion slope to increase systematically with p_T, while at lower p_T the resonances cause T^π to be smaller. In going to peripheral collisions a small decrease in the mean inverse slopes $\Delta T^{\pi^-} = -10$ MeV and $\Delta T^{\bar{p}} = -50$ MeV for approximate consistency with $p\bar{p}$ data [18] is introduced.

Larger inverse slope for baryon arises from smaller junction trajectory = higher effective string tension (three times higher) in limited pt-range (prior to quenching)

Standard fragmentation vs junction transport
Vitev, Gyulassy, PRC 65, 041902 (2003)

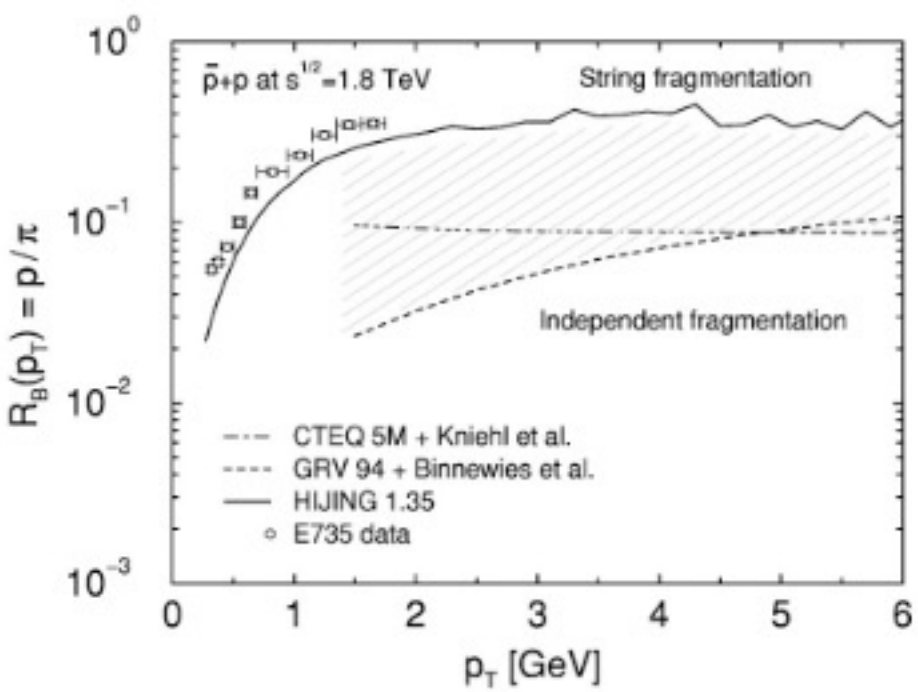

FIG. 1. The ratio $R_B \approx (p+\bar{p})/(\pi^+ + \pi^-)$ is shown for $p\bar{p}$ at $\sqrt{s} = 1.8$ TeV as a function of p_T. Low p_T FNAL E735 data [18] are shown for comparison. String fragmentation of minijets via HIJING1.35 [11] is also shown.

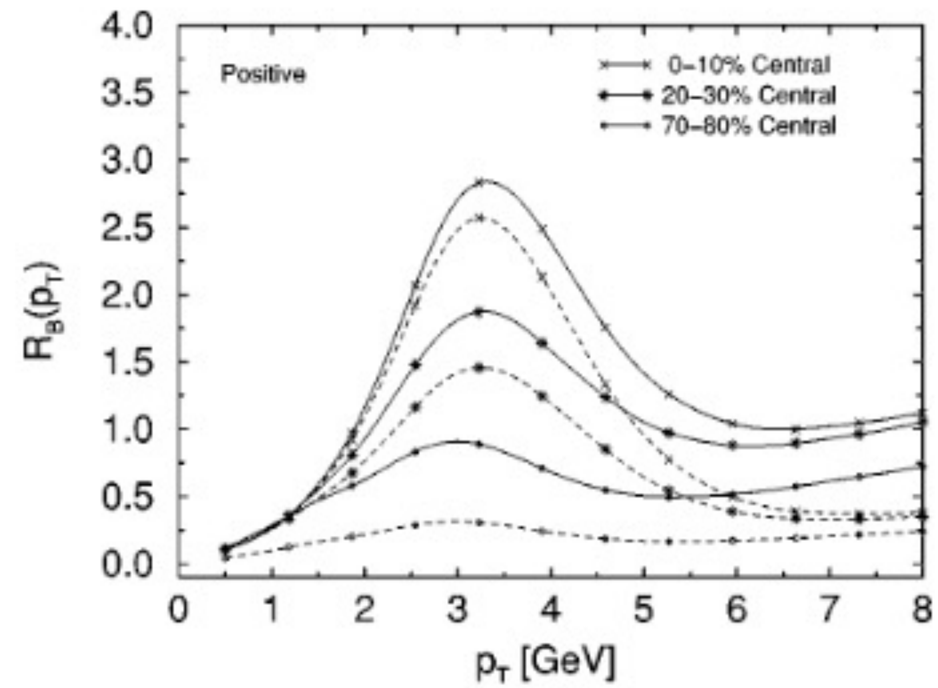

FIG. 4. The centrality and p_T dependence of the p/π^+ ratio is predicted for the same centrality classes as in Fig. 3. The solid (dashed) lines compare the difference between N_{part} ($N_{part}^{4/3}$) scaling of the junction component and 3(1)× the quenched fragmentation component as in Fig. 3.

Test

Baryon anomaly vs HIJING-Bbbar
PRC70, 064906 (2004)

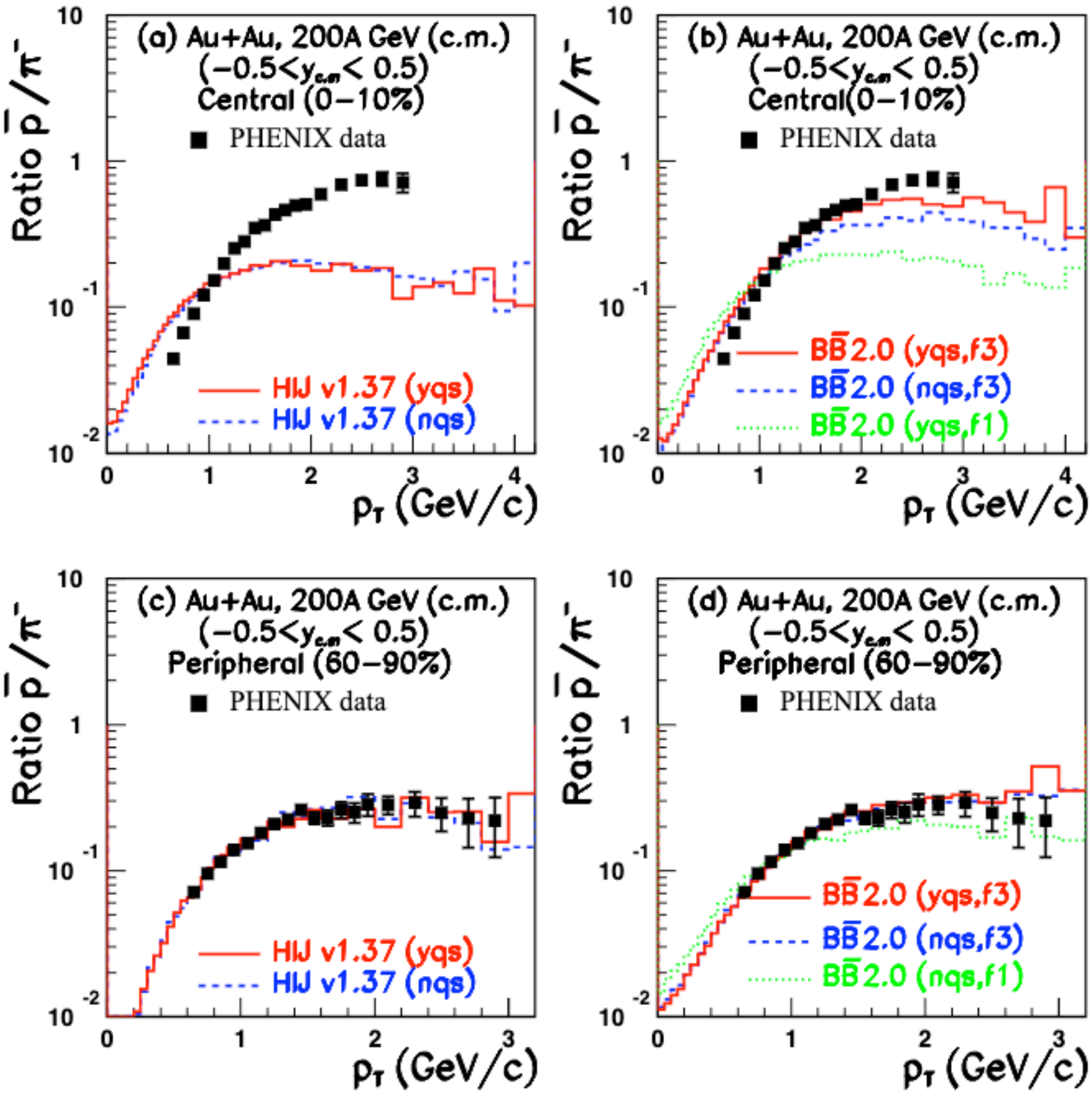

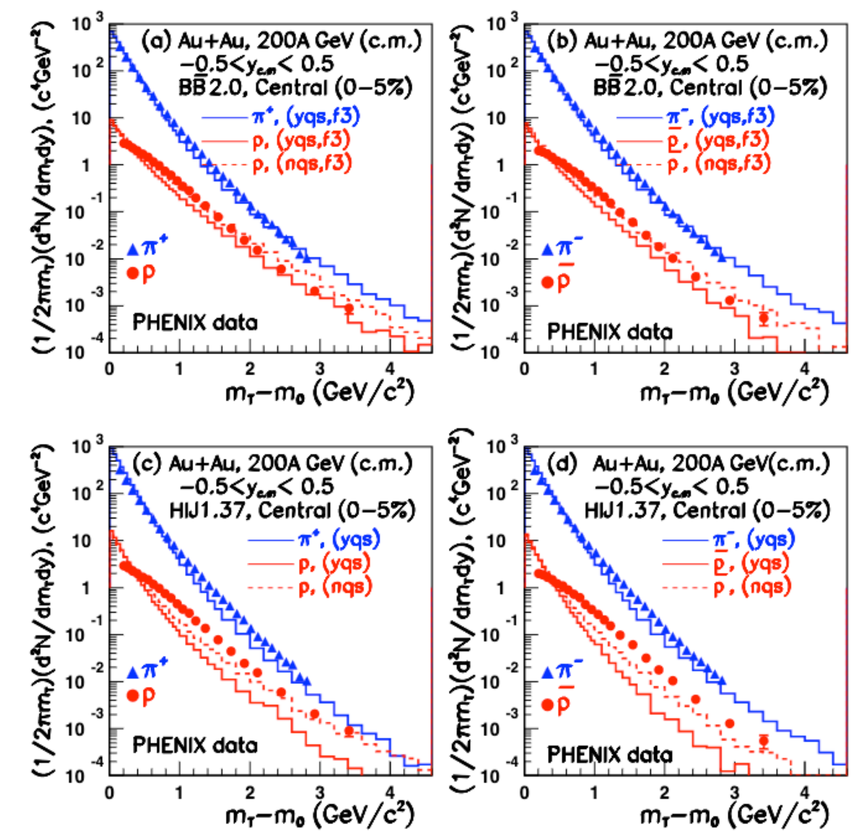

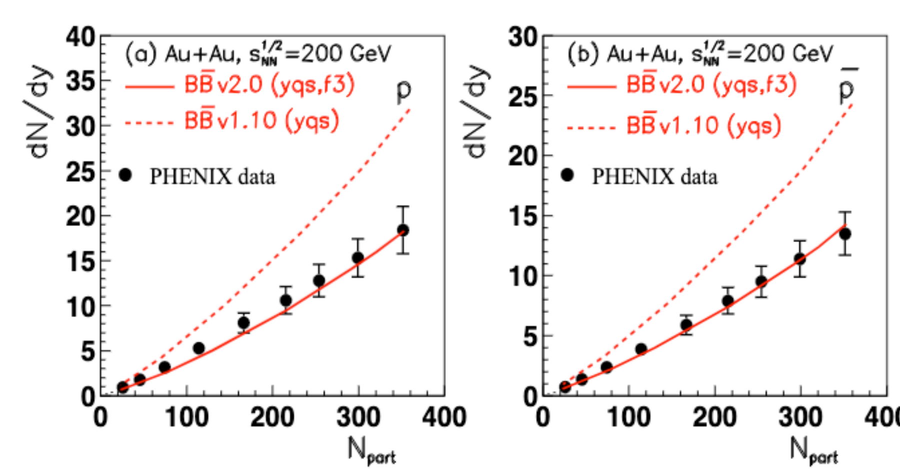

yqs/nqs = w./w.o. shadowing and quenching
f3 = enhanced string fragmentation, SCF)

Summary

Many of the early phenomena at SPS and RHIC could be explained with ‘the right’ implementation of gluon junctions:

1.) baryon transport
2.) hyperon enhancement
3.) hyperon to anti-hyperon ratios
4.) proton/pion ‘anomaly’ and R_{AA} differences between species

The right implementation had several ‘free’ parameters:

- Not only junctions (J) but also JJbar loops
- Di-quark suppression factor
- Shadowing and quenching mechanisms (yqs/nqs)
- String tension to parametrize strong color fields (SCF)
- Enhanced di-quark p_T kick (f=3)